

Studies on DC Magnetron Sputtered AZO Thin Films for HIT Solar Cell Application

Ranjitha R.*, T.K. Subramanyam, S. Pavan kumar, Nagesh M.

Interdisciplinary Research Centre, R.V. College of Engineering, 560059 Bengaluru, India

(Received 17 February 2020; revised manuscript received 11 April 2020; published online 25 April 2020)

Aluminum doped zinc oxide (AZO) is becoming an important and alternative transparent conducting oxide (TCO) material for solar photovoltaic applications due to its good electrical and optical characteristics, lower cost and more abundance, non-toxicity and stability in hydrogen plasma when compared to the popular indium tin oxide (ITO). In this work, AZO films are deposited on glass and silicon substrates with direct current (DC) magnetron sputtering using 5N pure Zinc Oxide target doped with 2 wt% Al₂O₃. The effect of deposition conditions on the structural, electrical and optical properties of the AZO films are investigated. The results demonstrated that the measured thickness of the deposited films are in the range 135-490 nm. The X-ray diffraction studies reveal that the AZO films exhibit hexagonal-wurtzite structure with the preferred orientation of grains along the (002) planes and an average crystal size of ~42 nm. At optimized sputter deposition parameters of an electrode distance of ~60 mm, substrate temperature of ~200 °C, target DC power of ~150 W and working pressure of ~2·10⁻³ mbar; the AZO films have shown an electrical resistivity of 1.27·10⁻³ Ω·cm and an average optical transmittance value of 83.76% in the visible range for an optimal film thickness of ~265 nm. Finally HIT Solar Cells with AZO/p-a-Si:H/i-Si:H/n-c-Si/n-a-Si:H/Al structure have been fabricated by applying the optimized AZO films as front transparent electrodes. It is observed from the preliminary experiments that the fabricated cells have shown an initial photo conversion efficiency of 10.18% with an open circuit voltage (V_{oc}) of 890 mV, short circuit current density (J_{sc}) of 15.68 mA/cm² and a fill factor (FF) of ~73%.

Keywords: AZO thin films, DC sputtering, HIT cells.

DOI: [10.21272/jnep.12\(2\).02037](https://doi.org/10.21272/jnep.12(2).02037)

PACS numbers: 84.60.Jt, 84.40.Fe

1. INTRODUCTION

In the present scenario the transparent conductive oxide (TCO) thin films are attracting researchers, because of their wide ranges of applications in solar cells, flat panel display devices, photovoltaic devices, etc. [1]. These TCO's are the wide band gap semiconductors ($E_g > 3.1$ eV) that have, high reflectance in the infrared region, high electrical conductivity with low resistivity (10^{-3} to 10^{-4} Ω·cm), and good optical transmittance of about 80-90% in the visible range, by considering all these properties, TCO materials are used in thin film solar applications for improving the performance of the HIT solar cells [1-2]. The various properties of TCO material strongly depend upon stoichiometric deviation, nature and quantity of impurities that are trapped in the host lattice [3]. Solar cells operate in the visible wavelength range of TCO films to minimize the photon absorption and reduce resistive loss. TCO being an one of the important layer in solar cell, plays a role of electrodes as well as antireflection films by providing low absorption and high conductivity properties [4] (SnO₂)-Tin oxide, (ITO)-Indium tin oxide, and (ZnO)-doped Zinc oxide are some of the well known Transparent Conducting Oxide materials, which can satisfy the above mentioned requirements [5]. Al in Zinc Oxide, Sn in indium oxide and Sb in tin oxide are commonly used impurities for good electrical and optical properties [6]. When compared to SnO₂, doped-ZnO is widely used as TCO due its low material cost, non-toxicity, high crystalline and stability in hydrogen plasma [7]. Currently transparent conductive films such as; ITO, ZnO-doped with Al, Ga etc. are used as the window layers in high efficiency silicon-based heterojunction solar cells [8]. ZnO thin

films are n-type semiconductors with intrinsic defects, such as interstitial zinc atoms and oxygen vacancies. The electrical conductivity of ZnO film is increased by doping with group III elements, such as; Boron, Aluminum, indium and Gallium. Doping is one of the most effective processes to improve the structure and properties of the materials [6] it is basically the introduction of the impurities into the semiconductors and this doping semiconductor materials are known as the extrinsic semiconductors. Therefore ZnO with Al dopant has been chosen as an appropriate TCO material which in turn minimizes the lattices defects and improves the electrical conductivity of HIT Solar Cell. The various techniques such as radio-frequency (RF) magnetron sputtering, direct-current (DC) magnetron sputtering, molecular beam epitaxy, pulsed laser deposition, electron beam evaporation, and the sol-gel process are used in doping of Zinc oxide with III group elements [5]. In this study we are choosing DC sputtering method for the deposition of Aluminum doped Zinc Oxide (AZO) thin films on the silicon wafers and glass substrates for studying the optical and electrical properties of the deposited samples.

The amorphous/crystalline silicon (a-Si/c-Si) heterojunction (HJ) solar cell has become one of the most effective solutions for the photovoltaic market due to their high stability, high conversion efficiencies and low temperature processing which leads to a reduction of fabrication cost in comparison with the high temperature diffused homo-junction technology [11]. Fig. 1 shows the a stacking structure of TCO/ a-Si:H(p)/a-Si:H(i)/c-Si(n)/a-Si:H(i)/a-Si:H(n+)/Al layer. The HIT solar cell, stands for Heterojunction intrinsic thin layer Solar Cell

* ranjitha0792@gmail.com

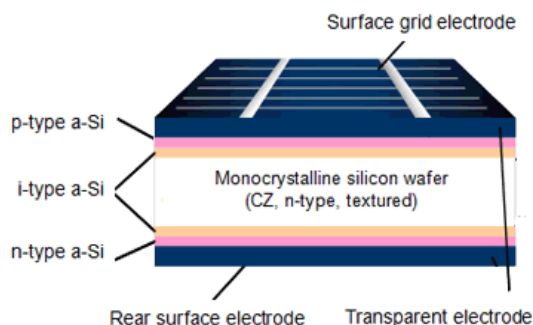


Fig. 1 – Schematic of HIT Solar Cell

which is composed of intrinsic (i-type) a-Si layer, (p-type) a-Si layer deposited on the n-type mono thin crystalline silicon wafer which is surrounded by ultra-thin amorphous silicon layers to form p/n heterojunction and i-type and n-type a-Si layers are deposited on the opposite side of n-type crystalline silicon wafer for back surface field. Thus hydrogenated *i/p* layer stack forms the emitter at the front side and a hydrogenated *i/n* layer stack forms the back-surface field [13]. On the top of the p-type a-Si layer transparent conducting oxide (TCO) layer has been deposited and then metal electrodes are fabricated on both the sides of the HIT Cell. The high quality intrinsic a-Si:H layer inserted between c-Si wafer and p-a-Si:H layer acts as an effective surface passivation layer for the c-Si wafer. The *p+/n+* doped a-Si layers functions as an effective emitter/Back surface field for the HIT Solar Cell. The transparent conductive oxide (TCO) layer has been deposited on top of the structure in order to improve the collection of sun light, to perform as antireflection layer and to provide a less resistive path to transport photo-generated charge carriers to the metal contacts [11]. Thus structural, electrical and optical behavior of the TCO layer influences the performance of the HIT solar cells which are explained in further sections.

2. EXPERIMENTAL DETAILS

Aluminum doped Zinc oxide (AZO) thin films are deposited using 5N pure Zinc Oxide target doped with 2 wt% Al₂O₃ by DC magnetron sputtering. The magnetron sputtering System consists of flexible magnetrons which are used to adjust the target-substrate distance and focus the angle of magnetron towards the substrate. The substrates are mechanically fixed on the rotatable steel work holder with substrate heater, which can provide a substrate temperature of about 300 °C and rotational speed of 60 rpm for optimizing the films. During the deposition process initial base pressure of about $\sim 5 \cdot 10^{-6}$ mbar is obtained using Turbo-Rotary based pump. The AZO films to be deposited on the HIT solar cells are initially deposited on the glass substrates for analyzing and optimizing the structural, electrical and optical properties of the deposited AZO films and then the best optimum results with process parameters are chosen and deposited on the front contact of the HIT solar cells. Before initializing the experiment the glass substrates are cleaned with standard cleaning procedure and then placed into sputtering chamber for the deposition of AZO films at a

working pressure of $\sim 2 \cdot 10^{-3}$ mbar. The experimental parameters implemented in this study are given in the Table 1 .

Table 1 – Deposition Parameters of AZO films by DC Magnetron Sputtering

Method of Deposition	DC magnetron Sputtering
Power Rating	1.5 kW DC Power, 600 V, 2.5 A
Sputter Target	5N pure, 98 wt% ZnO: 2 wt% Al ₂ O ₃
Base Pressure	$5 \cdot 10^{-6}$ mbar
Flow rate of Argon Gas	45 sccm
Working pressure	$2 \cdot 10^{-3}$ mbar
Electrode distance	60 mm
Substrate temperature	200 °C
DC power	50-250 W
Deposition time	15-30 mins

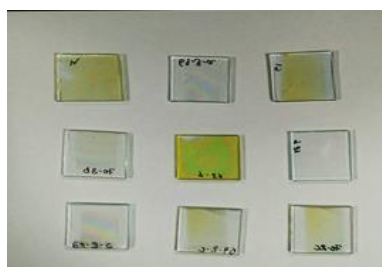


Fig. 2 – Deposited AZO films

Thickness of the deposited AZO films are measured using stylus profiler of Veeco-Dektak 6M model) and found to be in the range 135 nm to 490 nm with increasing target power from 50 to 250 W. The crystalline structure of the films are investigated using a Shimadzu maxima-7000 X-ray diffractometer (XRD) in which CuK_{α} radiation wavelength = 1.54182 Å. Electrical properties of the films are determined by using four-point probe method. Optical spectra of the films were recorded using UV-VIS spectrophotometer (Perkin Elmer Lambda 35) in the wavelength range of 300-2500 nm.

3. RESULTS AND DISCUSSION

In order to study the effect of DC power, AZO thin films were deposited on glass substrates with set parameters such as 60 mm of electrode distance, 200 °C substrate temperature, Ar gas flow rate of 45 sccm, by maintaining a working pressure of $\sim 2 \cdot 10^{-3}$ mbar. As shown in the Fig. 3 the deposition rate increased from 8.6 to 25.3 nm/min with the increase of DC power from 50 to 250 W. As the target power increases, the

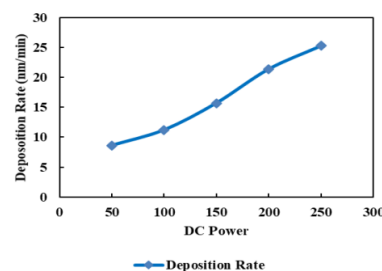


Fig. 3 – Effect of DC power on Rate of deposition

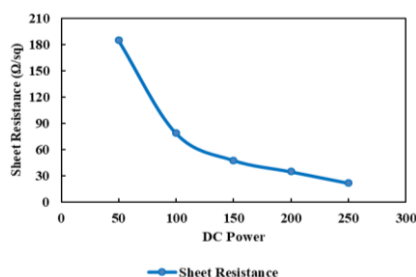


Fig. 4 – The effect of DC power on Sheet Resistance

sputtered atoms gain higher energy resulting with high surface mobility which enhances the film growth [9].

On the other hand, from the Fig. 4, the sheet resistance of the films decreased drastically for initial values then after almost saturated for further increase of sputtering power. The low resistance might be attributed to increase the grain size, which reduces the boundary scattering, also helps in improvement of crystal quality [10]. From the above experiments, an optimal target power value of 150 W has been chosen by considering the stability of the plasma during sputtering and hence a moderate sputter yield of ~ 15 nm/min is obtained.

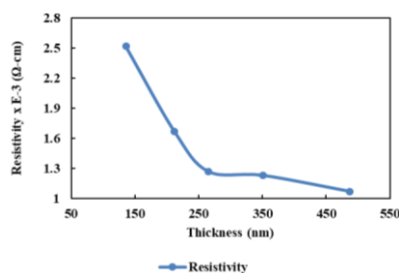


Fig. 5–Dependence of resistivity and thickness on DC power

The electrical properties of the AZO films as a function of DC power were characterized by four-point probe measurements at room temperature and was found to be varying from $2.52 \cdot 10^{-3}$ to $1.23 \cdot 10^{-3} \Omega \cdot \text{cm}$, with the increasing of the DC power from 50 to 250 W and then gets almost saturated for higher power as shown in the Fig. 5. This is because at higher power, negative oxygen ions accelerate towards the substrate and the deposited films become more stoichiometric which also enhances film crystallization and surface diffusion of the atoms with kinetic energy. Therefore the minimum resistivity value of $1.27 \cdot 10^{-3} \Omega \cdot \text{cm}$ has been considered as an optimized value for the sample deposited at 150 W.

Surface morphology of AZO deposited films are

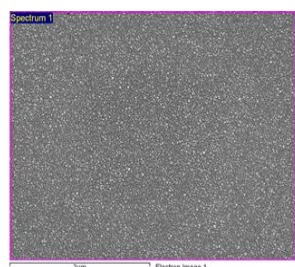


Fig. 6 – SEM image of the optimized AZO film studied using a Scanning Electron Microscope (SEM)

with 2 kV electron Voltage; 100Kx Magnification; 200 nm scale. The Fig. 6 shows the SEM image of the deposited AZO film which resulted with a grain size in the range of 35 nm to 50 nm and with an average grain size of ~ 42 nm. The crystals have seems to grown close to each other approximately with the same size, therefore from the above study we understand that the grain size has increased for the increase of the film thickness and on the other hand the sheet resistance of the films has been decreased which could be due to improvement in the crystallinity of the films.

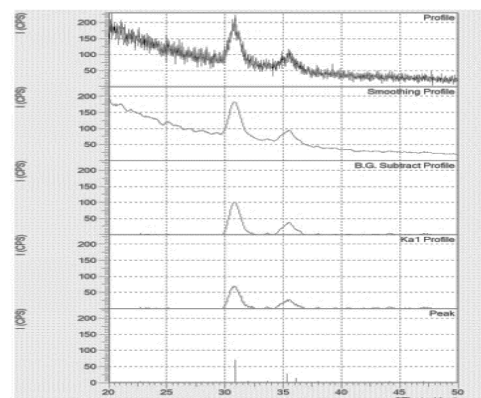


Fig. 7 – XRD Spectra of AZO films with respect to process temperature

The effect of substrate temperature on the properties of the AZO films is studied using X-ray diffractometer (Shimadzu maxima-7000) with Cu K_{α} are the radiation wavelength = 1.54182 \AA . The Fig.7 illustrates the X-ray diffraction property of AZO films, deposited at different substrate temperatures. The structural patterns of the deposited AZO films revealed major peaks at $2\theta = 0.8$ and 35.4 deg represents 002 and 101 planes respectively which indicate that as the substrate temperature increased, the average crystal size and diffraction peak intensity has also increased.

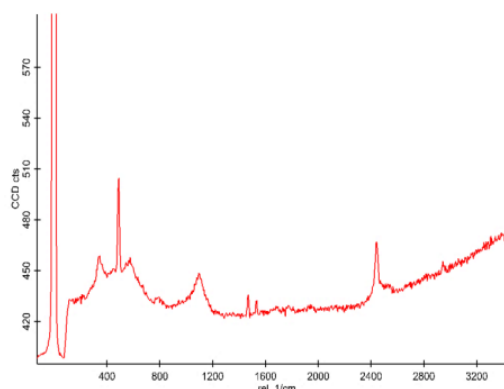


Fig. 8 – Raman Spectrum of AZO film

Raman spectrum of deposited AZO film was analyzed using the Raman spectrometer with the wavelength of 532 nm excitation laser source. Fig. 8 shows that the Raman spectrum of the AZO film and the peak observed at 500 cm^{-1} .

The optical transmission spectra of the AZO films are measured using a UV-VIS- NIR Spectrophotometer and are in the visible wavelength region of 300 nm to

1500 nm, as shown in the Fig. 9 The influence of DC power on the optical properties are investigated. The average % transmission calculated over the visible region was in the range of 81-85% with the increase of DC power from 50 W to 150 W and has decreased further for higher DC power.

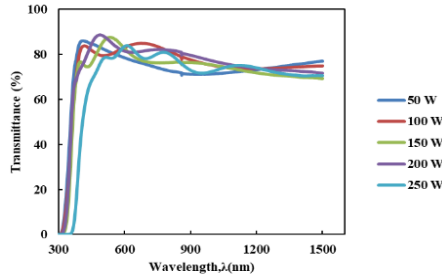


Fig. 9 – Optical transmittance spectra of AZO thin films deposited for different DC power

The effect of target power on electrical and optical properties of the deposited films clearly indicates that average optical transmittance has decreased from ~ 85% to 78% and on the other hand the sheet resistance has also decreased with respect to increase of the target DC power this is shown in the Fig. 4 Therefore, the above results are correlated to the formation of non-stoichiometric AZO films at higher deposition rates/target powers resulting films with more absorbing/reflecting in nature due to higher metallic content in the films [14].

The optical coefficient near the absorption edge can be calculated from transmission spectrum according to the equation $\alpha = 1/d \ln(I_0/I)$ Where d is the film thickness, I_0 is the intensity of the incident light and I is the intensity of the transmitted light.

The optical band gap of the films has been derived by Tauc plots from the absorption coefficient (α) which is calculated from the % transmission i.e $\alpha = -2 \log(\%T)$.

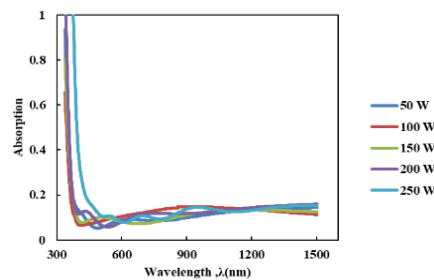


Fig. 10 – Optical absorption spectra of AZO thin films deposited for different DC power

The Tauc formula is as shown below:

$$(\alpha h \nu)^{1/2} = B \cdot (h \nu - E_g)$$

where, the quantity $h \nu$ (the energy of the light) is on the x axis and $(\alpha h \nu)^{1/2}$ is on the y -axis, and α is the absorption coefficient of wavelength and B constant.

The calculated band gap of the deposited AZO films has been reduced from 3.22 to 3.07 with respect to increase of DC power from 50 W to 250 W. The maximum band gap value of 3.16 eV is chosen as an optimum value

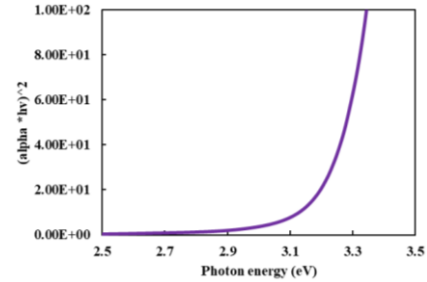


Fig. 11 – Optical band gap energy of optimized AZO film

for film thickness of 265 nm at DC power of 150 W which is shown in the Fig. 11. Thus from the above characterization results, The AZO films with thickness of ~ 265 nm, resistivity of $\sim 1.27 \cdot 10^{-3} \Omega \cdot \text{cm}$, transmittance of ~ 83.76%, and band gap of ~ 3.16 eV at DC power of 150 W are chosen as an optimum values for the deposition of AZO film on the front contact of the fabricated HIT Solar Cells.

3.1 Fabrication of HIT Solar Cell

The a-Si:H HIT Solar cells have been fabricated using plasma enhanced chemical vapour deposition system (RF-PECVD) which is fully automated through SCADA software integrated with PLC/user interface. It has 5 process chambers for deposition of individual layers, each chamber has electrode-gas shower facility connected to 300 W RF power supply with integrated network, substrate heater, dry pump for maintaining the process pressure, and Turbo-Roots-Rotary pumping system has been connected to central chamber for creating a base pressure of $\sim 5 \cdot 10^{-6}$ mbar.

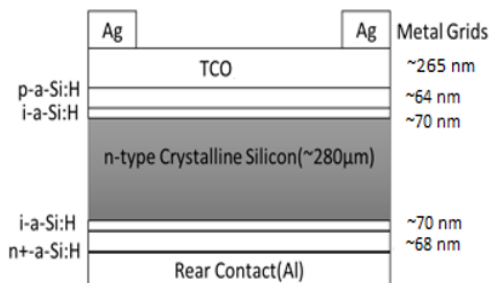


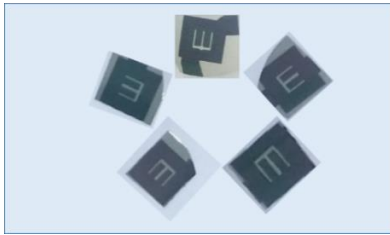
Fig.12 – Structure of HIT Solar Cell with layer details

High quality floating zone (FZ) n -type crystalline wafers are subjected to wafer cleaning and HF dip to remove any contaminants and native oxides and to passivate the surface with hydrogen. The cleaned wafers are then transferred to PECVD multi-chamber for deposition of $p-i-n$ layers with the process parameters as mentioned in the Table. 2 the process gases used are SiH_4 for the intrinsic layer, and SiH_4 along H_2 mixed with B_2H_6 and CH_4 for p -layer deposition and PH_3 for n -layer deposition. The dopant level of the doped p/n layers can be adjusted by changing the flow of the dopant gas. In this study, the process conditions such as an electrode distance of 25 mm and substrate temperature of 250 °C have been maintained constants, but varying the other process parameters such as dilution ratios, rate of deposition and operating pressures and RF power as shown below.

Table 2 – Experimental parameters of *p-i-n* layer optimization

Parameters	<i>i</i> -layer	<i>p</i> -layer	<i>n</i> -layer
Power (W)	7-10	7-10	7-10
Time (min)	5-30	5-30	5-30
Pressure (torr)	1	1	1
Process gases used for layer deposition with gas flow rate (sccm)	H ₂ (0-150) SiH ₄ (5-10)	H ₂ (0-150) SiH ₄ (2-6) B ₂ H ₆ (2-10) CH ₄ (5-10)	H ₂ (0-150) PH ₃ +SiH ₄ (5-10)

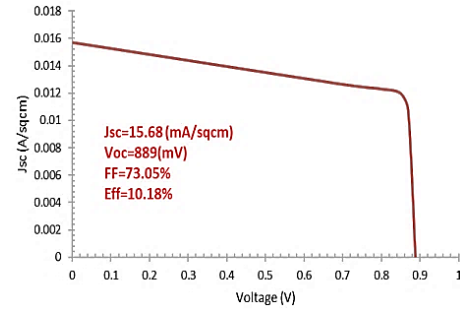
Initially (intrinsic) *i*-layer has been deposited on the *n*-type crystalline silicon wafer by varying the process parameters as mentioned in the Table 2. The *p*-layer is deposited on the (intrinsic) *i*-layer for creating *p/i*-junction (front emitter layer), and then *n*-layer has been deposited on the opposite side of the *n*-type crystalline silicon wafer on the intrinsic *i*-layer for back surface field. Then the (TCO) Aluminum doped-Zinc Oxide film is deposited on the front contact of the *p*-layer and metal (Al) electrodes are deposited using Thermal Evaporation on both the sides of the fabricated HIT Solar Cell. The results obtained are tabulated in Table 3.

**Fig. 13** – Fabricated HIT Solar Cells**Table 3** – Optimized layer properties used for HIT Solar Cell properties

Device layers	Optimum Results of Individual layers
<i>i</i> -layer	Dark Conductivity = $2.78 \cdot 10^{-10} \text{ S}\cdot\text{cm}^{-1}$ Photo Conductivity = $9.20 \cdot 10^{-5} \text{ S}\cdot\text{cm}^{-1}$ Photo Gain = $3.31 \cdot 10^5$ Band Gap = 1.88 eV Thickness ~ 70 nm
<i>p</i> -layer	Conductivity = $3.08 \cdot 10^{-6} \text{ S}\cdot\text{cm}^{-1}$ Band Gap = 1.97 eV Thickness ~ 64 nm
<i>n</i> -layer	Conductivity = $1.66 \cdot 10^{-2} \text{ S}\cdot\text{cm}^{-1}$ Band Gap = 1.73 eV Min. Thickness ~ 68 nm
TCO-layer	Grain size ~ 42 nm, Resistivity = $1.27 \cdot 10^{-3} \Omega\cdot\text{cm}$, Transmittance ~ 83.76%, Band gap ~ 3.16 eV
Metal Contact	Thickness = 300 nm

REFERENCES

- Joseph George, Robert Haley, Brian Pate, Steve Rozeveld, Mitchell Krafft, Mark T. Bernius, Simon Yeung, *34th IEEE Photovoltaic Specialists Conference (PVSC)*, 000440-000444 (2009).
- Shadia J. Ikhmayies, *Transparent Conducting Oxides for Solar Cell Applications* (Ed. by A. Sayigh) (Springer International Publishing: Switzerland: 2017).
- S.U. Lee, J.-H. Boo, B. Hong, *Jpn. J. Appl. Phys.* **50**,

**Fig. 14** – Current-Voltage characteristics of the fabricated HIT Solar Cell

The fabricated HIT solar Cells after deposition of optimized AZO films and metal electrodes are subjected for *I-V* Measurements using *I-V* System with AM1.5 equivalent Light Source and resulted with an initial photo conversion efficiency of 10.18% with an open circuit voltage (V_{oc}) of 890 mV, short circuit current density (J_{sc}) of 15.68 mA/cm² and a fill factor (FF) of ~ 73% illustrated in Fig. 14. The J_{sc} is measured to know the amount of light passing through the TCO films and reaching the solar cell [12].

V_{oc} is to monitor the impact of the sputtering process on the a-Si emitter, fill factor depends on the thickness of the *p*-layer and conversion efficiency increases with respect to decrease of thickness of *p-i-n* layers of the HIT solar cell [4].

4. CONCLUSION

The Aluminum doped zinc oxide (AZO) thin films are sputtered using 5N pure Zinc Oxide target doped with 2 wt% Al₂O₃ by maintaining constant target-substrate distance, substrate temperature and varying the target DC power. The measured thicknesses of the deposited films are in the range of 135 nm to 490 nm. The optimized AZO films exhibited an average optical transmission of ~ 83.76%, band gap of 3.16 eV, resistivity of $1.27 \cdot 10^{-3} \Omega\cdot\text{cm}$ and thickness ~ 265 nm for a set of process parameters; DC power = 150 W, argon flow = 45 sccm, sputtering pressure of $\sim 2 \cdot 10^{-3}$ mbar. This optimized AZO film is deposited on the front contact of the HIT solar Cell to study the *I-V* characteristics using *I-V* System with AM1.5 equivalent Light Source resulted with an open circuit voltage (V_{oc}) of 890mV, short circuit current density (J_{sc}) of 15.68 mA/cm², fill factor (FF) of ~73% and a photo conversion efficiency of 10.18%.

ACKNOWLEDGEMENTS

The authors are grateful to the Solar Energy Research Initiative (SERI), Department of Science and Technology, New Delhi, and the Management of R.V. College of Engineering, Bangalore for executing this research work.

- 01AB10 (2011).
4. S. Fernandez, F.B. Naranjo, *Sol. Energy Mater. Sol. C.* **94** No 2, 157 (2010).
5. Chien-Yi Peng, Mohammad M. Hamasha Daniel VanHart, Susan Lu, Charles R. Westgate, *IEEE T. Dev. Mater. Reliability* **13**, No 1, 236 (2013).
6. Yanli Liu, Yufang Li, Haibo Zeng, *J. Nanomater.* 196521 (2013).
7. Mohit Agarwal, Rajiv O Dusane, *IEEE 44th Photovoltaic Specialist Conference (PVSC)*, 18221200 (2017).
8. Yuqi Chen, *IOP Conf. Series: Materials Science and Engineering*, **423**, 012170 (2018).
9. Kyunghwan Kim, HyungWook Choi, *J. Korean Phys. Soc.* **55** No 5, 1945 (2009).
10. Yu Qiu, I. Gordon, *Mater. Chem. Phys.* **141**, 744 (2013).
11. Z. Bensaad, *Int. J. Multidiscip. Educ. Res.* **6** No 22
12. Lahcen Nkhaili, Abdelkader El'kissani, *Eur. Phys. J. Appl. Phys.* **66**, 30302 (2014).
13. Ayse Seyhan, Tolga Altan, Omer Can Ecer, *J. Phys.: Conf. Ser.* **902**, 012024 (2017).
14. T.K. Subramanyam, P. Goutham, S. Pavan Kumar, *Mater. Today: Proc.* **5**, 10851 (2018)